

## Preparation and Properties of Carbon Fiber/Si<sub>3</sub>N<sub>4</sub> Composites

WANG He-Yun<sup>1,2</sup>, LIU Qian<sup>1</sup>, ZHOU Yao<sup>1,2</sup>, ZHOU Zhen-Zhen<sup>1</sup>, LIU Guang-Hui<sup>1</sup>

(1. State Key Laboratory of High Performance Ceramics and Superfine Microstructure, Shanghai Institute of Ceramics, Chinese Academy of Sciences, Shanghai 200050, China; 2. University of Chinese Academy of Sciences, Beijing 100049, China)

**Abstract:** To investigate the effects of carbon fiber (C<sub>f</sub>) adding content on the properties of Si<sub>3</sub>N<sub>4</sub>, C<sub>f</sub>/Si<sub>3</sub>N<sub>4</sub> composites with 0, 2wt% and 5wt% of short carbon fibers were prepared by hot-press sintering method, using Y<sub>2</sub>O<sub>3</sub> as sintering additives. With long-time ball milling process, carbon fibers were well dispersed in mixed powders using ethanol as dispersion medium. Carbon fibers distribute uniformly in the composites and Si<sub>3</sub>N<sub>4</sub> grains grow to a certain degree in the vertical direction to the pressure of hot-press. The interfacial by-product silicon carbide (SiC) phase forms due to the reaction between added C<sub>f</sub> and Si<sub>3</sub>N<sub>4</sub> particles or SiO<sub>2</sub> layer on surface of Si<sub>3</sub>N<sub>4</sub> particles during high temperature sintering. The sample with 2wt% C<sub>f</sub> addition achieves a higher value of thermal conductivity (45.8 W/(m·K)), while the thermal conductivity of Si<sub>3</sub>N<sub>4</sub> without C<sub>f</sub> is only 37.1 W/(m·K). Therefore, the addition of C<sub>f</sub> can improve the thermal conductivity of the composites. The fracture toughness of the composites has a slight increase with C<sub>f</sub> adding. The measured hardness values for all samples are within a range of 16.6–16.8 GPa.

**Key words:** C<sub>f</sub>/Si<sub>3</sub>N<sub>4</sub> composite; hot-press sintering; interfacial reaction; thermal conductivity; mechanical property

Si<sub>3</sub>N<sub>4</sub> ceramic is not only an important engineering ceramics with a variety of applications<sup>[1]</sup>, but also a promising substrate and package material for high power integrated circuits due to its good thermal conductivity, high electrical resistivity, low dielectric constant, and low thermal expansion coefficient<sup>[2]</sup>. However, the thermal conductivity of Si<sub>3</sub>N<sub>4</sub> is still not high enough to be used in some industrial areas. In recent decade years, more and more researches focused on the improvement of thermal conductivity of Si<sub>3</sub>N<sub>4</sub>. It has been found that the thermal properties of Si<sub>3</sub>N<sub>4</sub> are strongly influenced by the quality of raw powders<sup>[3-4]</sup>, type of sintering aids<sup>[5]</sup>, forming technique<sup>[6]</sup>, sintering method<sup>[7-8]</sup>, and sintering conditions<sup>[9]</sup>. But few investigations on the thermal properties of Si<sub>3</sub>N<sub>4</sub>-based composites, second-phase composited, or fiber composited Si<sub>3</sub>N<sub>4</sub> have been reported.

Since carbon fiber materials were discovered, enormous amount of research interests have been sparked due to their potential applications as reinforcement components. One promising usage of carbon fibers is to act as fillers in composite materials to improve their thermal, electrical, and mechanical performances. Some carbon fibers have very good thermal properties. For example, the mesophase-pitch-based carbon fibers have a high thermal conductivity of 500 W/(m·K); the graphitized carbon fibers have a

higher thermal conductivity. Therefore, C<sub>f</sub> was used to improve the thermal properties of composites. Due to the addition of C<sub>f</sub>, the thermal conductivities of carbon fiber-in-oil suspensions<sup>[10]</sup> and carbon fiber-in-polymer composites were enhanced<sup>[11]</sup> significantly. Borrell<sup>[12]</sup> reported that an increase of 83% in thermal conductivity at room temperature was observed when adding 80vol% of carbon nanofibers to ZrO<sub>2</sub> ceramics.

In our present study, the high-density C<sub>f</sub>/Si<sub>3</sub>N<sub>4</sub> composites were tried to be fabricated by hot-press sintering with rod-like Si<sub>3</sub>N<sub>4</sub> particles as raw powders and short carbon fibers as reinforcement. The interfacial structure between C<sub>f</sub> and Si<sub>3</sub>N<sub>4</sub> matrix was investigated and the effect of C<sub>f</sub> addition on the thermal conductivity and mechanical properties of C<sub>f</sub>/Si<sub>3</sub>N<sub>4</sub> were discussed, respectively.

## 1 Experiment

### 1.1 Preparations

The rod-like raw powders of Si<sub>3</sub>N<sub>4</sub> were prepared *via* partial nitridation and self-propagating high temperature synthesis process (SHS)<sup>[13]</sup>. The image of rod-like Si<sub>3</sub>N<sub>4</sub> powders was shown in Fig. 1(a). The rod-like Si<sub>3</sub>N<sub>4</sub> powder is a mixture of  $\alpha$ - and  $\beta$ -phase (seen in Fig. 2). The carbon fibers were purchased from Japan (Toray Industries

Received date: 2014-04-02; Modified date: 2014-05-23; Published online: 2014-06-20

Foundation item: Science and Technology Committee of Shanghai Municipal Government (11JC1413600)

Biography: WANG He-Yun(1990–), female, candidate of master degree. E-mail: wangheyun@student.sic.ac.cn

Corresponding author: LIU Qian, professor. E-mail: qianliu@sunm.shcnc.ac.cn

CO., Ltd.) and its diameter is 7–8  $\mu\text{m}$  (seen in Fig. 1(b)). For better dispersion, the carbon fibers were cut into a length less than 100  $\mu\text{m}$ . The raw  $\text{Si}_3\text{N}_4$  powders were mixed with 3wt%  $\text{Y}_2\text{O}_3$  (purity>99.9%, Yuelong New Materials Co., Ltd, Shanghai, China) in ethanol using  $\text{Si}_3\text{N}_4$  balls in a polyethylene pot. After 24 h milling, the short  $\text{C}_f$  (varied in 0–5wt%) was added to the batches. After milling for another 12 h to reach a uniform dispersion of  $\text{C}_f$ , the slurry was dried at 80 $^\circ\text{C}$  for 10 h and sieved through an 80-mesh screen. The mixed powders were then placed into a graphite container (25 mm in diameter) and hot-pressed at 1800 $^\circ\text{C}$  for 2 h, under a uniaxial pressure of 30 MPa in a flowing  $\text{N}_2$  atmosphere. Three types of composite samples with different carbon fiber content (0, 2wt%, 5wt%) were obtained, defined as SN-Cf-0, SN-Cf-2, and SN-Cf-5, respectively.

## 1.2 Characterization

The phase compositions of  $\text{C}_f/\text{Si}_3\text{N}_4$  specimens were analyzed by XRD with  $\text{CuK}\alpha$  radiation ( $\lambda=0.1541$  nm, a D/MAX-2550VX X-ray diffractometer working at 40 kV and 100 mA). The microstructures of the starting powder morphology and fracture surface of bulk samples were observed by a field emission scanning electron microscope (FESEM, JSM-6700 JEOL, Japan, 10.0 kV). The interfacial structure between  $\text{C}_f$  and  $\text{Si}_3\text{N}_4$  matrix was characterized by a high-resolution transmission electron microscope (HRTEM, JEM2100F JEOL, Japan, 200 kV) coupled with a selected area electron diffractometer (SAED) and energy-dispersive spectroscopy (EDS) using Cu-grid as sample holder.

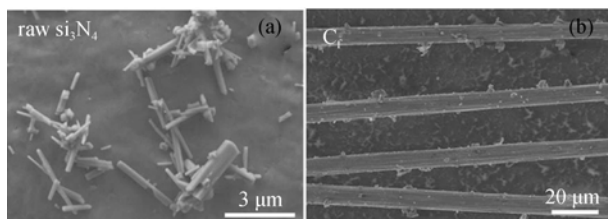


Fig. 1 SEM images of raw  $\text{Si}_3\text{N}_4$  particles (a) and raw carbon fibers (b)

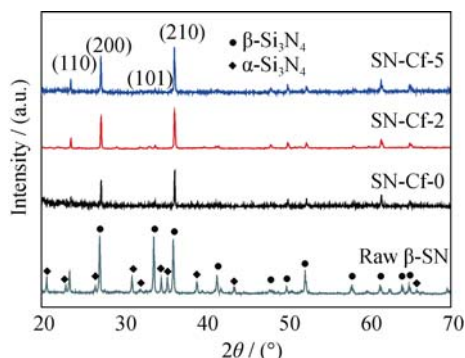


Fig. 2 XRD patterns of raw  $\text{Si}_3\text{N}_4$  powders and  $\text{C}_f/\text{Si}_3\text{N}_4$  composites

Thermal conductivity ( $k$ ) was calculated by the equation of  $k=\rho C_p \alpha$ , where  $\rho$ ,  $C_p$  and  $\alpha$  represent the bulk density, specific heat, and thermal diffusivity of the disk specimen, respectively. While the bulk density ( $\rho$ ) was measured by the Archimedes method in distilled water, the thermal diffusivity ( $\alpha$ ) was measured by a laser-flash method (LFA427) from room temperature (RT) to 500 $^\circ\text{C}$  on disk specimens with 10 mm in diameter and 2 mm in thickness, and the specific heat ( $C_p$ ) was measured with a differential scanning calorimeter (DSC) in RT–500 $^\circ\text{C}$  temperature range. The hardness ( $H_v$ ) and fracture toughness ( $K_{IC}$ ) were also measured by Vickers indentation method at a load of 4.9 N for 10 s at RT. All the measured surfaces of samples were vertical to the direction of axial pressure applied in hot-press procedure.

## 2 Results and discussion

### 2.1 Phase formation and distribution in $\text{C}_f/\text{Si}_3\text{N}_4$ composites

It is believed that  $\beta\text{-Si}_3\text{N}_4$  as main phase is beneficial for obtaining high thermal-conduction and mechanical property. The XRD patterns of prepared  $\text{C}_f/\text{Si}_3\text{N}_4$  composite specimens with different  $\text{C}_f$  concentration (seen in Fig. 2) show that there is only  $\beta\text{-Si}_3\text{N}_4$  main phase in the three samples of SN-Cf-0, SN-Cf-2, and SN-Cf-5. In comparison, obvious signs of  $\alpha\text{-Si}_3\text{N}_4$  phase are shown in raw  $\text{Si}_3\text{N}_4$  powders. It is found that a nearly complete phase-transformation from  $\alpha\text{-Si}_3\text{N}_4$  to  $\beta\text{-Si}_3\text{N}_4$  occurred after 2 h sintering of  $\text{C}_f/\text{Si}_3\text{N}_4$ . Yang<sup>[14]</sup> reported that the existence of carbon would prohibit the  $\alpha\rightarrow\beta$   $\text{Si}_3\text{N}_4$  phase transformation. However, the carbon fibers in our research have almost no negative effect on  $\alpha$  to  $\beta$  transformation during sintering at high temperature of 1800 $^\circ\text{C}$ . All three composite specimens display an obvious orientation tendency of the matrix  $\text{Si}_3\text{N}_4$  grains, as identified in XRD patterns by a sharp difference in relative intensities of XRD peaks between composite samples and raw powders of  $\text{Si}_3\text{N}_4$ . For example, the XRD peaks of (101) plane for the characteristic  $\beta\text{-Si}_3\text{N}_4$  phase are almost not visible in the sintered samples while they are very strong for the raw powders. Such alignment of  $\beta\text{-Si}_3\text{N}_4$  grains is a result of the uniaxial pressure applied on the rod-like  $\text{Si}_3\text{N}_4$  raw powders packed in graphite die during hot pressing. Moreover, no  $\text{C}_f$  was detected by XRD. It's hard to judge whether carbon fiber additives can keep their natural state after sintering just by using XRD detection.

SEM and optical microscopy images of  $\text{C}_f/\text{Si}_3\text{N}_4$  composites are shown in Fig. 3. In all samples, considerable amount of elongated grains are observed in  $\text{Si}_3\text{N}_4$  matrix

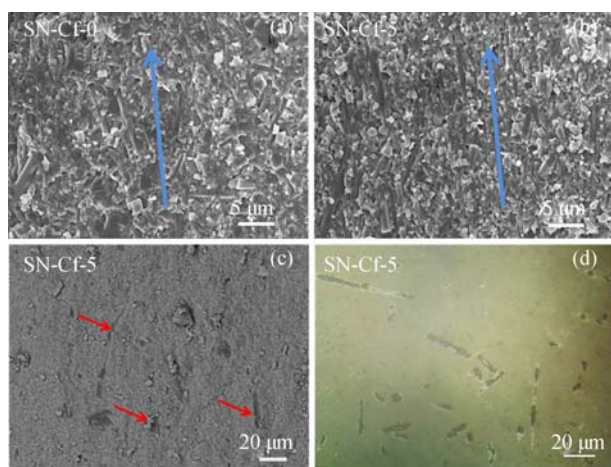


Fig. 3 SEM and optical microscopy images of C<sub>f</sub>/Si<sub>3</sub>N<sub>4</sub> Secondary electron image (SEI) of fracture surfaces of SN-Cf-0 (a) and SN-Cf-5 (b), back scattered electron image (BSEI) of fracture surface of SN-Cf-5 (c), and optical microscopy image of SN-Cf-5 surface (d)

with 1–2 μm in diameter, and the elongated grains are aligned to some degree, which is in agreement with the XRD results in which the alignment of β-Si<sub>3</sub>N<sub>4</sub> grains has been confirmed by the sharp peaks at (200) and (210) planes. The grain morphology in SN-Cf-2 sample is similar to that in SN-Cf-0 and SN-Cf-5, which is not shown here. In these images the carbon fibers in the dark contrast can be readily observed, as arrowed. Carbon fibers are well-distributed in Si<sub>3</sub>N<sub>4</sub> matrix (seen in Fig. 3(c) and Fig. 3(d)). In addition, the diameter of carbon fibers have been decreased to 5 μm when compared with that of the raw carbon fibers with diameter of 7–8 μm. It has been proved that the carbon fibers would be degraded by hot-pressing process at higher temperatures<sup>[15-16]</sup>.

## 2.2 Interface reaction between C<sub>f</sub> and Si<sub>3</sub>N<sub>4</sub> in C<sub>f</sub>/Si<sub>3</sub>N<sub>4</sub> composites

In the composites, the interface reaction often occurs between second-phase and matrix, leading to the formation of transition products at interface which may influence properties of composites. Based on the TEM observations of our C<sub>f</sub>/Si<sub>3</sub>N<sub>4</sub> samples, a typical interfacial microstructure of C<sub>f</sub>/Si<sub>3</sub>N<sub>4</sub> having 5wt% carbon fibers is shown in Fig. 4, with corresponding EDS patterns of different regions. The carbon fibers and Si<sub>3</sub>N<sub>4</sub> grains are easily identified as arrowed in Fig. 4(a). Additionally, a transition layer with 2 μm width can be observed between carbon fiber and Si<sub>3</sub>N<sub>4</sub> matrix. EDS patterns (Fig. 4(d)) show that the transition layer contains silicon, carbon, and a trace of oxygen element. Considering the degradation of carbon fibers and EDS patterns, it can be inferred that the transition layer is SiC phase caused by the carbothermal reduction reaction between Si<sub>3</sub>N<sub>4</sub> or SiO<sub>2</sub> existing on the Si<sub>3</sub>N<sub>4</sub> grain surface and carbon fibers at high temperatures.

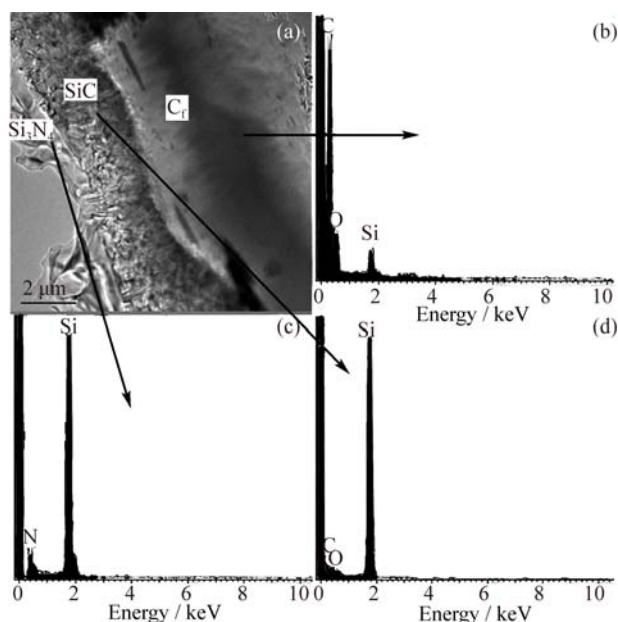
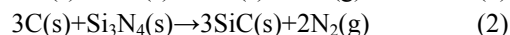
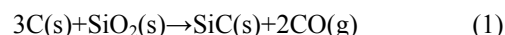


Fig. 4 TEM image of interfacial surface between C<sub>f</sub> and Si<sub>3</sub>N<sub>4</sub> in SN-Cf-5 (a) and EDS patterns of different regions (b, c, d) arrowed in (a)

The possible reaction routes are described as follows :



The reaction (1) is more preferably reached than that of reaction (2) in the Si<sub>3</sub>N<sub>4</sub>-SiO<sub>2</sub>-C system<sup>[17]</sup>, due to its lower reaction active energy. After the complete consumption of SiO<sub>2</sub> layer on Si<sub>3</sub>N<sub>4</sub> grain surface, the remained carbon will react with Si<sub>3</sub>N<sub>4</sub> via reaction (2). In general, these two reactions start at 1450°C, so the formation of transition layer of SiC phase may have happened at relatively low temperatures during hot-press sintering process. It was reported that Si<sub>3</sub>N<sub>4</sub>/SiC composites and SiC-based composites were successfully fabricated according to the carbothermal reaction (1) and (2)<sup>[14,17]</sup>.

TEM and HRTEM images of the interfacial transition layer of SiC are shown in Fig. 5. Many small SiC crystals are packed between C<sub>f</sub> and Si<sub>3</sub>N<sub>4</sub> matrix. The size of grains in the SiC transition layer is about 200 nm. Furthermore, SiC grains in the transition layer can be also identified by the interplanar *d*-spacing of 0.25 nm corresponding to the (111) plane of SiC phase and the corresponding SAED pattern is shown in Fig. 5(b). The formation of SiC particles by carbothermal reaction between Si<sub>3</sub>N<sub>4</sub> and carbon was also proved and reported by Choi<sup>[18]</sup>.

## 2.3 Thermal conductivity and mechanical property of C<sub>f</sub>/Si<sub>3</sub>N<sub>4</sub> composites

Addition of C<sub>f</sub> into Si<sub>3</sub>N<sub>4</sub> matrix exhibits some positive effects on thermal conductivity of composites in our research. Table 1 shows the thermal conductivity variation of C<sub>f</sub>/Si<sub>3</sub>N<sub>4</sub> composites with different concentration of car

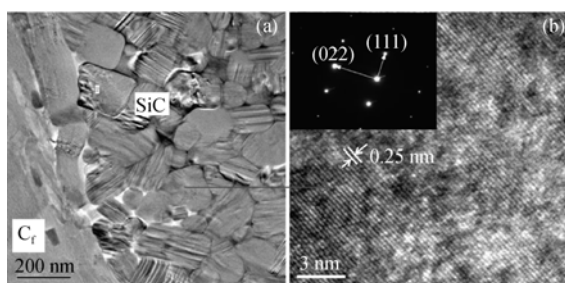


Fig. 5 TEM (a) and HRTEM (b) images of interfacial transition layer of SiC in SN-Cf-5 specimen

bon fibers measured at room temperature. The sample SN-Cf-2 shows the highest value of thermal conductivity up to 45.8 W/(m·K), while the value of  $\text{Si}_3\text{N}_4$  without  $\text{C}_f$  addition is only 37.1 W/(m·K). Because the used Toray carbon fibers have a high thermal conductivity (80 W/(m·K)), the introduction of carbon fibers with 2wt% enhances the thermal conductivity of  $\text{Si}_3\text{N}_4$  matrix. A similar enhancement effect was also reported in carbon fibers/PMMA (polymethyl methacrylate) composites<sup>[19]</sup> and carbon nanotube/alumina composites<sup>[20]</sup>. It showed that the introduction of carbon materials into the matrixes with low thermal conductivity effectively improve the thermal properties of the composites. But the key factor is the uniform dispersion of carbons in matrix. In our experiments, a well-dispersed  $\text{C}_f$  in matrix is realized by using ethanol as efficient dispersion medium with long-time ball-milling, as shown in Fig. 3.

Both thermal diffusivity and thermal conductivity of SN-Cf-5 are slight lower than that of SN-Cf-0. Based on the TEM microstructure observation of  $\text{C}_f/\text{Si}_3\text{N}_4$  composites, the lower thermal property of SN-Cf-5 is attributed to the interfacial reaction between  $\text{C}_f$  and matrix. In short, three factors, caused by the interfacial reaction, are responsible for the lower thermal properties. Firstly, there are SiC layers with 2  $\mu\text{m}$  in width between  $\text{C}_f$  and  $\text{Si}_3\text{N}_4$  grains in the composites, as shown in Fig. 4. The transition layers, composed of random SiC particles wrapping around the surface of  $\text{C}_f$  as protective shells, obstruct the heat flow between  $\text{C}_f$  and  $\text{Si}_3\text{N}_4$  grains. Secondly, the  $\text{C}_f$  degrade due to the carbothermal reduction reaction during high temperature sintering. As a result, the diameter of  $\text{C}_f$  was reduced from its original 7–8  $\mu\text{m}$  to 5–6  $\mu\text{m}$  in final

state by exhausting for the formation of SiC layer. The carbon fibers could not keep their integrity, which might make a negative effect on the thermal properties of composites. Thirdly, during sintering process, both carbothermal reduction reaction (1) and (2) can release gases ( $\text{CO}$  or  $\text{N}_2$ ), which cause many micropores in bulk samples. Moreover, the micropores will compromise a part of thermal conductivity by scattering the heat flow in composites. In SN-Cf-5 sample, the obvious degradation of carbon fibers resulted in the production of more nano-size SiC grain layers, more lattice defects, and more micropores at interface regions, compared with SN-Cf-2 sample, which finally leads to a lower thermal conductivity.

The evolution of thermal conductivity with varied temperatures for the composite materials is shown in Fig. 6. The thermal conductivity of the three ceramic samples decreases gradually with the temperature increasing from room temperature to 500°C. This is the typical behavior for polycrystalline materials, demonstrating that phonon disharmony-induced degrades thermal conductivity at high temperatures<sup>[21]</sup>.

The results of hardness ( $H_v$ ) and fracture toughness ( $K_{IC}$ ) measurements of  $\text{C}_f/\text{Si}_3\text{N}_4$  composites are shown in Table 2. The mechanical properties of the  $\text{Si}_3\text{N}_4$  matrix are not improved significantly by the introduction of carbon fibers. The fracture toughness of SN-Cf-0, SN-Cf-2 and SN-Cf-5 is 5.0, 4.9 and 5.3  $\text{MPa}\cdot\text{m}^{1/2}$ , respectively, and the hardness values are all within a range of 16.6–16.8 GPa. From SEM observations of sample SN-Cf-5 (Fig. 3), the pullout mechanism of reinforcement from short carbon fiber intrusion is not obvious. It means that the fracture toughness enhancement owing to the exhaustion of fracture energy from the pullout of fibers does not work in the duration of indentation experiment of  $H_v$  and  $K_{IC}$  measurements. Furthermore, it is believed that the carbon fibers did not bear a large part of load in the hardness measurement procedure and the to the degradation and

Table 1 Thermal properties of  $\text{C}_f/\text{Si}_3\text{N}_4$  composites measured at room temperature

Composites	$\text{C}_f$ /wt%	$\rho$ /( $\text{g}\cdot\text{cm}^{-3}$ )	$C_p$ /( $\text{mm}^2\cdot\text{s}^{-1}$ )	$\alpha$ /( $\text{J}\cdot\text{g}^{-1}\cdot\text{K}^{-1}$ )	$k$ /( $\text{W}\cdot\text{m}^{-1}\cdot\text{K}^{-1}$ )
SN-Cf-0	0	3.27	17.98	0.59	37.12
SN-Cf-2	2	3.31	19.99	0.61	45.84
SN-Cf-5	5	3.28	15.12	0.58	33.43

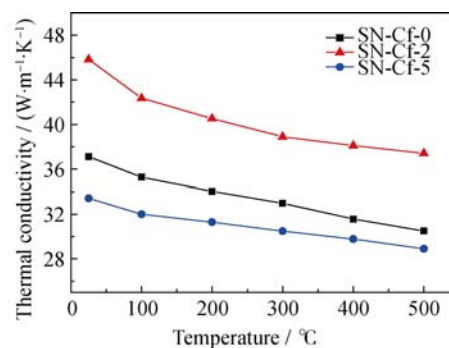


Fig. 6 Variation of thermal conductivity with temperature for  $\text{C}_f/\text{Si}_3\text{N}_4$  composites



**Table 2** Mechanical property of C<sub>f</sub>/Si<sub>3</sub>N<sub>4</sub> composites measured at room temperature

Composites	C <sub>f</sub> /wt%	H <sub>v</sub> /GPa	K <sub>IC</sub> /(MPa·m <sup>1/2</sup> )
SN-Cf-0	0	16.6	5.0
SN-Cf-2	2	16.8	4.9
SN-Cf-5	5	16.8	5.3

short length of carbon fibers added. Therefore, the values of  $H_v$  keep a nearly constant one. If the degradation of carbon fiber can be inhibited by optimizing the sintering conditions or resisted by coating the fibers to stop interfacial reaction, or the length of additional carbon fiber can be tailored properly, the thermal conductivity and mechanical properties of C<sub>f</sub>/Si<sub>3</sub>N<sub>4</sub> would be enhanced effectively. Further researches are needed to be proceeded to declare the fundamental understanding and optimize the processing.

### 3 Conclusion

In summary, the oriented silicon nitride based composites with different addition (0, 2wt% and 5wt%) of carbon fibers (C<sub>f</sub>) were prepared by hot-press sintering method at 1800°C. The C<sub>f</sub> reacts with Si<sub>3</sub>N<sub>4</sub> (or SiO<sub>2</sub> on Si<sub>3</sub>N<sub>4</sub> grain surfaces) at interface during sintering process via a carbothermal reduction reaction. As a result, a thick transition SiC layer is formed at the interface between C<sub>f</sub> and Si<sub>3</sub>N<sub>4</sub> matrix. A higher value of thermal conductivity, 45.8 W/(m·K), belongs to the sample containing the 2wt% C<sub>f</sub> concentration. The addition of C<sub>f</sub> can improve the thermal conductivity of the composites, while the interfacial reaction between C<sub>f</sub> and Si<sub>3</sub>N<sub>4</sub> matrix contributes the deterioration of thermal conductivity. The thermal conduction improvement is balanced by the content of C<sub>f</sub> addition and the degree of C<sub>f</sub> deterioration. In addition, the influence of C<sub>f</sub> fillers on the improvement the mechanical properties ( $H_v$  and  $K_{IC}$ ) are not very obvious, due to the degradation and short length of carbon fibers as well.

### ACKNOWLEDGMENTS

Many thanks for supplying of rod-like Si<sub>3</sub>N<sub>4</sub> powders from Prof. Yuping Zeng's group, Structural Ceramics Engineering Research Center, Shanghai Institute of Ceramics. Many thanks to Dr. Xingang Wang of the State Key Laboratory of High Performance Ceramics and Superfine Microstructure for his useful discussion and help in hot-press sintering experiments.

### References:

- [1] KRSTIC ZORAN, KRSTIC D. VLADIMIR. Silicon nitride: the engineering material of the future. *Journal of Materials Science*, 2011, **47**(2): 535–552.
- [2] WATARI KOJI. High thermal conductivity non-oxide ceramics. *Journal of the Ceramic Society of Japan*, 2001, **109**(1): S7–S16.
- [3] PENG MENG-MENG, NING XIAO-SHAN. Sintering of β-Si<sub>3</sub>N<sub>4</sub> powder and thermal conductivity of the ceramic. *Rare Metal Materials and Engineering*, 2013, **42**(1): 405–408.
- [4] ZHANG YING-WEI, YU JIAN-BO, XIA YONG-FENG, *et al.* Microstructure and mechanical performance of silicon nitride ceramic with seeds addition. *Journal of Inorganic Materials*, 2012, **27**(8): 807–812.
- [5] ZHU XIN-WEN, ZHOU YOU, HIRAO KIYOSHI. Effects of processing method and additive composition on microstructure and thermal conductivity of Si<sub>3</sub>N<sub>4</sub> ceramics. *Journal of the European Ceramic Society*, 2006, **26**: 711–718.
- [6] ZHU XIN-WEN, ZHOU YOU, HIRAO KIYOSHI. Post-densification behavior of reaction-bonded silicon nitride (RBSN): effect of various characteristics of RBSN. *Journal of Materials Science*, 2004, **39**(18): 5785–5797.
- [7] WARARI KOJI, HIRAO KIYOSHI, BRITO E MANUEL, *et al.* Hot isostatic pressing to increase thermal conductivity of Si<sub>3</sub>N<sub>4</sub> ceramics. *Journal of Materials Research*, 1998, **14**(4): 1538–1551.
- [8] WATARI KOJI, HIRAO KIYOSHI, TORIYAMA MOTOHIRO. Effect of grain size on the thermal conductivity of Si<sub>3</sub>N<sub>4</sub>. *Journal of the American Ceramic Society*, 1999, **82**(3): 777–779.
- [9] ZHOU YOU, HYUGA HIDEKI, KUSANO DAI, *et al.* A tough silicon nitride ceramic with high thermal conductivity. *Advanced Materials*, 2011, **23**(39): 4563–4567.
- [10] CHOI Stephen U S, ZHANG Z G, YU W, *et al.* Anomalous thermal conductivity enhancement in nanotube suspensions. *Applied Physics Letters*, 2001, **79**(14): 2252–2254.
- [11] HAN SEUNGJIN, CHUNG D D L. Increasing the through-thickness thermal conductivity of carbon fiber polymer-matrix composite by curing pressure increase and filler incorporation. *Composites Science and Technology*, 2011, **71**(16): 1944–1952.
- [12] BORRELL B, ROCHA V G, TORRECILLAS R, *et al.* Effect of carbon nanofibers content on thermal properties of ceramic nanocomposites. *Journal of Composite Materials*, 2011, **46**(10): 1229–1234.
- [13] YAO DONG-XU, XIA YONG-FENG, ZOU KAI-HUI, *et al.* Porous Si<sub>3</sub>N<sub>4</sub> ceramics prepared via partial nitridation and SHS. *Journal of the European Ceramic Society*, 2013, **33**(2): 371–374.
- [14] YANG JIAN-FENG, ZHANG GUO-JUN, KONDO NAOKI, *et al.*

- Synthesis and properties of porous  $\text{Si}_3\text{N}_4/\text{SiC}$  nanocomposites by carbothermal reaction between  $\text{Si}_3\text{N}_4$  and carbon. *Acta Materialia*, 2002, **50**(19): 4831–4840.
- [15] WANG XIAO-YAN, ZHU DONG-MEI, LI PENG, *et al.* Behavior of short carbon fibers in  $\text{C}_{\text{fiber}}/\text{Si}_3\text{N}_4$  composites by hot pressed sintering. *Journal of Reinforced Plastics and Composites*, 2009, **28**(2): 167–173.
- [16] MAGNANT J, PAILLER R, PETITCORPS Y L, *et al.* Fiber-reinforced ceramic matrix composites processed by a hybrid technique based on chemical vapor infiltration, slurry impregnation and spark plasma sintering. *Journal of the European Ceramic Society*, 2013, **33**(1): 181–190.
- [17] YANG JIAN-FENG, ZHANG GUO-JUN, KONDO NAOKI, *et al.* Porous 2H-silicon carbide ceramics fabricated by carbothermal reaction between silicon nitride and carbon. *Journal of the American Ceramic Society*, 2003, **86**(6): 910–914.
- [18] CHOI JAE-YOUNG, KIM CHONG-HEE, KIM DO-KYUNG, *et al.* Carbothermic synthesis of monodispersed spherical  $\text{Si}_3\text{N}_4/\text{SiC}$  nanocomposite powder. *Journal of the American Ceramic Society*, 1999, **82**(10): 2665–2671.
- [19] ELIMAT Z M, HUSSAIN W T, ZIHLIF A M. PAN-based carbon fibers/PMMA composites: thermal, dielectric, and DC electrical properties. *Journal of Materials Science: Materials in Electronics*, 2012, **23**(12): 2117–2122.
- [20] KUMARI L, ZHANG T, DU G H, *et al.* Thermal properties of CNT-alumina nanocomposites. *Composites Science and Technology*, 2008, **68**(9): 2178–2183.
- [21] BAKSHI SRINIVAS R, BALANI KANTESH, AGARWAL ARVIND. Thermal conductivity of plasma-sprayed aluminum oxide-multiwalled carbon nanotube composites. *Journal of the American Ceramic Society*, 2008, **91**(3): 942–947.

## 碳纤维复合 $\text{Si}_3\text{N}_4$ 陶瓷材料的制备及性能研究

王贺云<sup>1,2</sup>, 刘 茜<sup>1</sup>, 周 遥<sup>1,2</sup>, 周真真<sup>1</sup>, 刘光辉<sup>1</sup>

(1. 中国科学院 上海硅酸盐研究所, 高性能陶瓷和超微结构国家重点实验室, 上海 200050; 2. 中国科学院大学, 北京 100049)

**摘 要:** 为研究碳纤维( $\text{C}_f$ )加入量对复合材料性能的影响, 本研究以  $\text{Y}_2\text{O}_3$  为烧结助剂, 采用热压烧结技术制备了  $\text{C}_f/\text{Si}_3\text{N}_4$  复合材料, 其中碳纤维加入量为 0、2wt% 和 5wt%。选用乙醇作分散介质, 通过球磨工艺可有效分散短切碳纤维。研究表明: 碳纤维在复合材料中分散均匀, 且材料中的晶粒在垂直于热压压力的方向呈现一定取向排列。高温烧结过程中, 碳纤维与  $\text{Si}_3\text{N}_4$  或其表面的  $\text{SiO}_2$  层发生反应, 生成  $\text{SiC}$  中间层。适量碳纤维加入有助于提高复合材料的热导性能。当  $\text{C}_f$  加入量为 2wt% 时,  $\text{C}_f/\text{Si}_3\text{N}_4$  的热导率较高, 为  $45.8 \text{ W}/(\text{m}\cdot\text{K})$ ; 而不添加  $\text{C}_f$  的样品, 其热导率为  $37.1 \text{ W}/(\text{m}\cdot\text{K})$ 。加入  $\text{C}_f$  后,  $\text{C}_f/\text{Si}_3\text{N}_4$  的断裂韧性有小幅提高, 维氏硬度在 16.6~16.8 GPa 范围内变化。

**关 键 词:**  $\text{C}_f/\text{Si}_3\text{N}_4$  复合材料; 热压烧结; 界面反应; 热导; 力学性能

中图分类号: TQ174

文献标识码: A